CHAPTER - III

DNA BINDING, AMELIORATION OF OXIDATIVE STRESS AND MOLECULAR DOCKING STUDY OF Zn(II) METAL COMPLEX OF A NEW SCHIFF BASE LIGAND

3.1. Introduction:

Molecules that interact with DNA have been studied extensively with the aim of designing new types of chemotherapy agents and probes for nucleic acid structures [1-2]. Studying the interaction of transition metal complexes with DNA have been the main focus of recent investigations. Cisplatin (cis-diamminedichloridoplatinum(II)) is the first clinically approved anticancer drug; its various analogues are found to be capable to bind to DNA, halting its replication and induce apoptosis [3]. However, these complexes have so many disadvantages: poor solubility [4], dose-limiting side effects like nausea, nephrotoxicity and neurotoxicity [5] and acquired resistance in many cancer types [6]. These basic problems associate with chemotherapy necessitate the evolvement of new anticancer approaches.

Development of new molecules that can obstruct cancerous cells by interacting with DNA in a non-classical mechanism is an example of new anticancer approach. Transition metal complexes are ideal for these tasks, as their unique characteristics allowing specific interactions with DNA and other important bio-molecules [7].Transition metals that are utilized extensively in these field include platinum [8], ruthenium [9], Zinc [10], titanium [11], rhodium [12], copper[13], palladium [14], gold [15], Vanadium [16] and iron [17]. Schiff base metal complexes have also gained recognition for their utilities in these biological processes [18]. In recent years, many studies associated with Schiff base metal complexes show promising anticancer activity and are of great interest in both chemistry and biology [19].

Zinc, which is known as “essential trace element” plays an important part in many biological processes. It is essential for the functionality of more than 300 enzymes and

Published in *J. Coord. Chem.*, 2018, 71 (14), 1-24.

vital for the stabilization of DNA, gene expression [20]. It is involved in immune responses, in homeostasis, in apoptosis and in ageing. Zn-binding proteins and enzymes are protective in stress, infections [21]. To explore the chemistry of Zn(II) complexes and DNA interaction, here we have synthesized and characterised a new Zn(II) complex and studied its interaction with Calf Thymus DNA(CT DNA) by different physical and spectroscopic techniques.

3.2. Experimental Section:

3.2.1. Synthesis of Schiff Base Ligand:

A hot ethanolic solution of 3, 3' Methylenedianiline (0.1mol) was refluxed with 2-hydroxy 5- nitro Benzaldehyde (0.2 mol) in a round bottom flask for 2h with constant stirring. The resulting yellow colored solid product was separated by filtration, washed with ethanol followed by diethyl ether and dried in vacuum desiccator over anhydrous calcium chloride.

3.2.2. Synthesis of Metal Complex:

Hot ethanolic solution of Zn(II) acetate was added dropwise to the equimolar ethanolic solution of synthesized ligand. The resulting mixture was then stirred and refluxed (at 40-50 °C) for 2 h whereupon the Zn(II) metal complex was precipitated out. The dark yellow colored solid complex was separated by filtration, washed with ethanol and dried in vacuum desiccator.

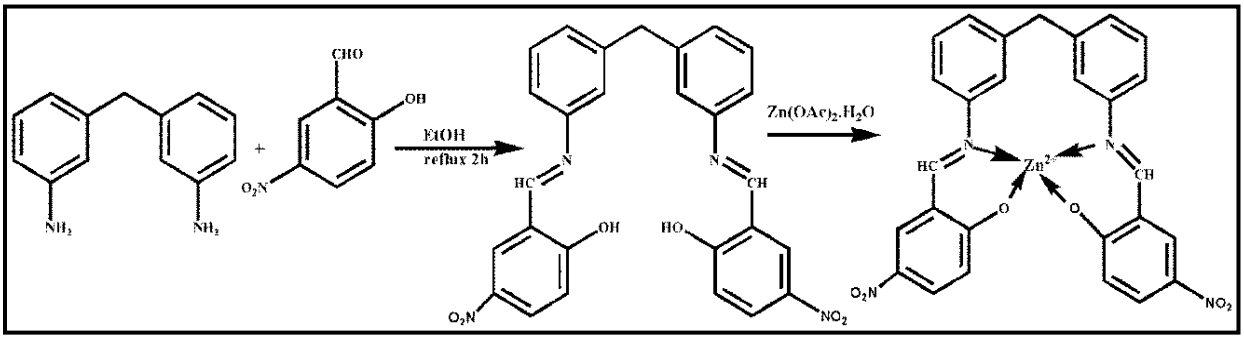

Scheme.3.1. Synthesis of schiff base ligand and its Zn(II) complex.

3.3. Results and Discussion:

The formation of the investigated Schiff base ligand and its metal complex is represented in Scheme.3.1.

3.3.1. Characterization of the ligand and its Zn(II) complex:

The synthesized ligand and its corresponding Zn(II) complex have been characterized by different analytical and spectroscopic techniques (IR, ^{1}H and ^{13}C NMR, UV-Visible, molar conductance *etc.*). The analytical data of the synthesized ligand and its Zn(II) complex along with physical properties is listed in Table 1. The ligand and the metal complex are moisture insensitive, air stable and soluble in DMSO and DMF. The analytical data are in good agreement with calculated values and are consistent with formation of mononuclear Zn(II) complex having metal to ligand ratio 1:1.

3.3.1.1. Molar Conductance:

The synthesized Zn(II) complex was dissolved in DMSO solvent and molar conductance of 10^{-3} mol dm^{-3} complex solution was measured at room temperature (Table 3.1.). The molar conductance value indicates that the metal complex is a non-electrolyte [28].

Table. 3.1. Analytical and Physical data of Schiff base ligand and its Zn(II) complex:

Compound	m.p. (◦C)	Colour (% yield)	Mol. Wt. (gm)	% Found (calcd.)			$\Lambda_m\ \Omega^{-1}\ mol^{-1}\ cm^2$
				C	H	N	
H_2L ($C_{27}H_{20}N_4O_6$)	140	Yellow (84)	496	65.71 (65.32)	4.16 (4.03)	11.13 (11.29)	_
[Zn(L)] ($C_{27}H_{18}N_4O_6Zn$)	>250	Dark Yellow (78)	559	58.06 (57.96)	3.41 (3.22)	9.94 (10.02)	14.11

3.3.1.2. Infrared Spectra:

The coordination of the ligand to the metal ion have been studied by comparing the IR data of the ligand with its Zn(II) complex. The IR spectra of synthesized Schiff base and its corresponding Zn(II) complex is shown in Fig.3.1. There are some appreciable shifts in the stretching frequencies of Zn(II) complex compared to free ligand. The Schiff base shows a characteristic strong band at 1618 cm^{-1}due to the azomethine ν(C=N) [28]. This band gets shifted to 1599 cm^{-1} in the synthesized complex indicating the participation of the azomethine nitrogen in complexation [28]. A broad band at 3447 cm^{-1} due to phenolic -OH group of ligand is disappeared in the corresponding Zn(II) complex suggesting the involvement of oxygen atom of -OH group in coordination to Zn(II) ion [28]. The coordination of O atom of phenolic -OH group to metal ion is further proved by the shift in ν(C-O) band of ligand at 1099 cm^{-1} to higher frequency at 1105 cm^{-1} in Zn(II) complex [29]. The participation of phenolic O and azomethine N in complexation are confirmed by the development of two non-ligand bands in the spectra of complex at 535 cm^{-1} and 466 cm^{-1} due to ν(Zn-O) and ν(Zn-N), respectively [28]. Therefore, the above arguments together with the elemental analyses indicated that Schiff base ligand behaves as a dibasic tetradentate ligand coordinated to the metal ion via the azomethine N and deprotonated phenolic O and the complex possibly have a tetrahedral geometry because of d^{10} configuration of Zn(II).

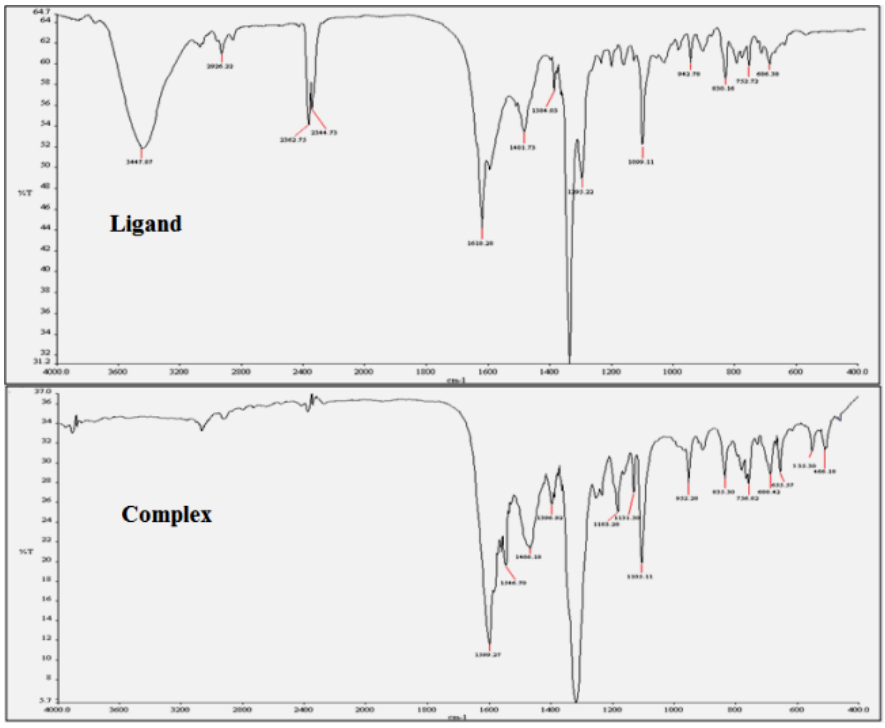

Fig.3.1. FTIR Spectra of the synthesized ligand and its Zn(II) complex.

3.3.1.3. NMR Spectra:

The ^{1}H NMR spectra of Schiff base ligand and its Zn(II) complex is shown in Fig.3.2. The synthesized Schiff base showed a singlet at δ 9.17 ppm because of azomethine proton (-CH=N-) [24]. However, in case of Zn(II) complex this -CH=N- peak is shifted to 8.70 ppm suggesting the involvement of azomethine nitrogen in coordination with Zn(II). Moreover, the ligand showed a signal at 10.29 ppm due to hydroxyl (-OH) proton which disappears in the synthesized complex revealing the deprotonation of –OH group during complexation [30].

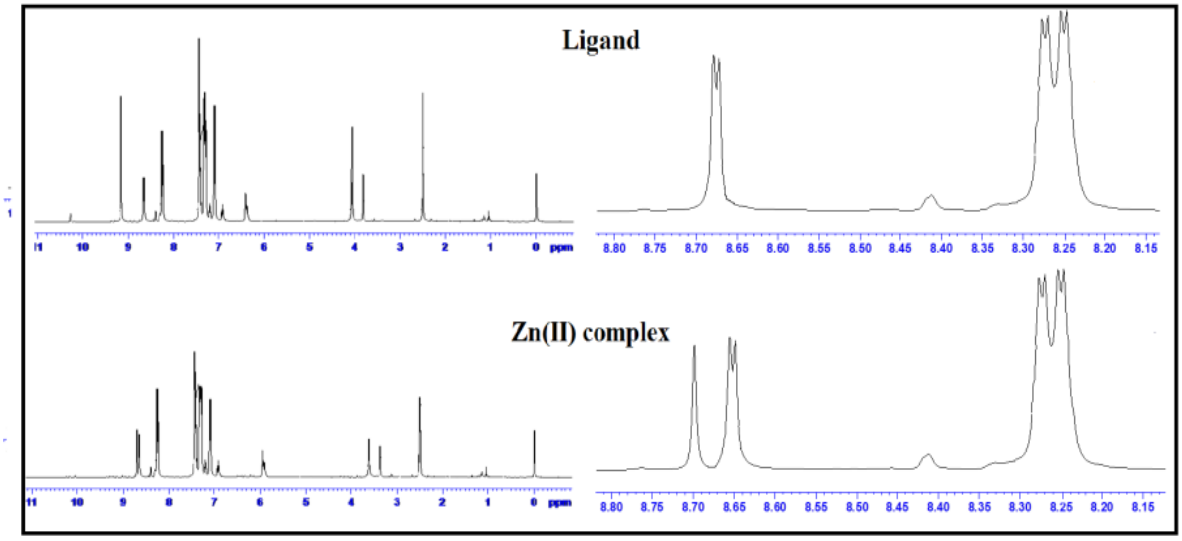

Fig.3.2. ^{1}H NMR spectrum of Schiff base ligand and its Zn(II) complex.

The ^{13}C NMR spectrum of both ligand and complex show peaks at 116.19-153.12 ppm for aromatic carbons and at 42.09 for -CH_2 (Fig.3.3.). The ligand signals at 167.71 ppm and 169.01 ppm for -CH=N and -C-OH group are shifted upfield to 160.03 ppm and 162.12 ppm for the Zn(II) complex. There are no appreciable changes in other peaks. So the changes in peak position for -CH=N and -C-OH carbons in the synthesized complex with respect to ligand confirms the complexation.

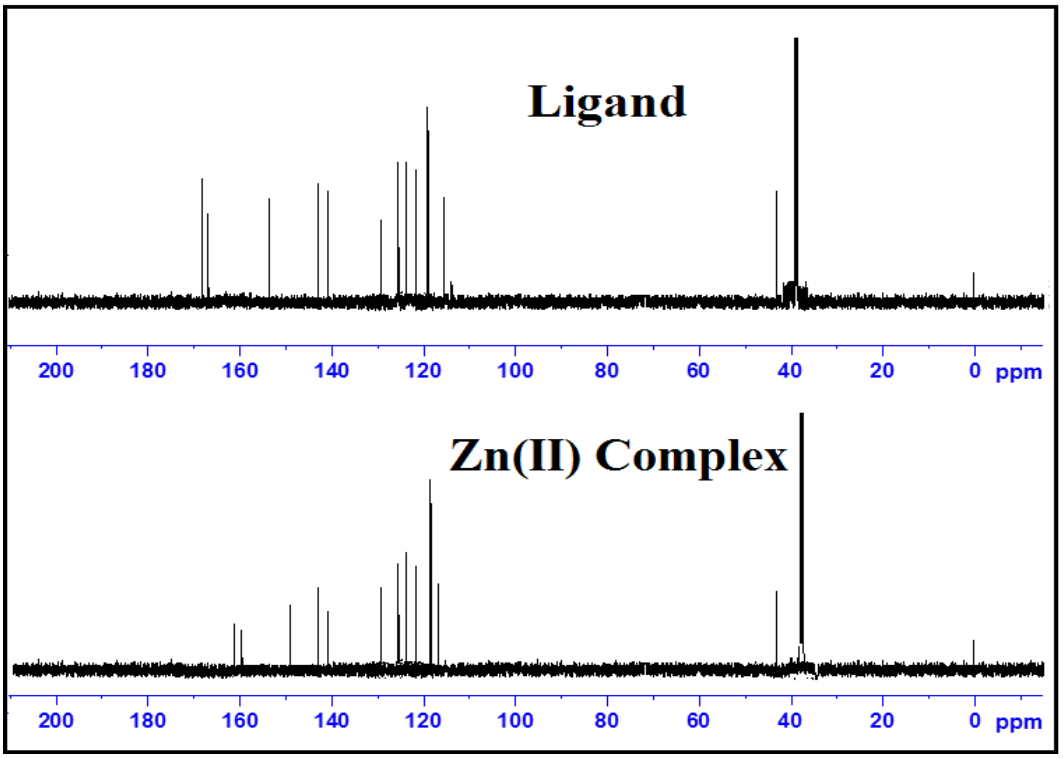

Fig.3.3. ^{13}C NMR spectrum of Schiff base ligand and its Zn(II) complex.

3.3.1.4. Electronic Spectra:

The UV-visible absorption spectra of the Schiff base and its Zn(II) complex were recorded in DMSO (1×10^{-5} M) at room temperature, depicted in Fig.3.4. The electronic absorption spectrum of Schiff base contains two bands at 380 and 430 nm. The band at higher energy (380 nm) is attributed to π-π* transitions of phenyl ring while the lower energy band at 430 nm is assigned to n-π* transition of azomethine (-CH=N-) group [30]. These absorption bands also exist in the spectrum of Zn(II) complex but undergoes blue shift. This shifts in the spectra of the synthesized complex supports the coordination of the ligand to Zn(II) ion. The Zn(II) complex because of its d^{10} configuration do not show any d-d transition and hence its diamagnetic and possibly having tetrahedral geometry.

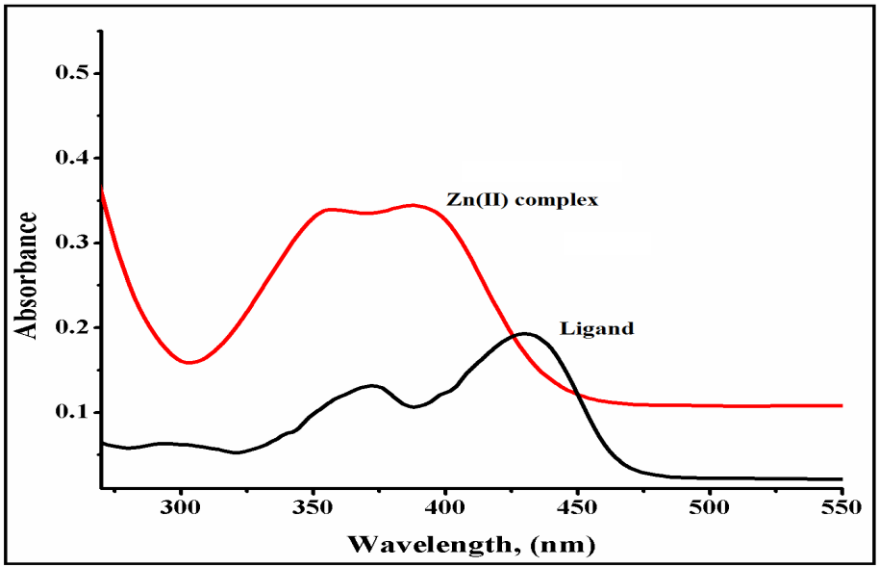

Fig. 3.4. UV-visible spectra of Synthesized ligand and its Zn(II) complex in DMSO.

3.3.2. DNA binding study:

3.3.2.1. Absorption study:

Electronic absorption spectroscopy serves as an effective tool to study the binding mode of DNA with metal complexes. The binding behavior of DNA to metal complex is often investigated by the changes in the wavelength and in the absorbance. A metal complex binds to DNA via intercalation usually results in bathochromism (red shift in wavelength) and hypochromism shift because of strong stacking interaction of DNA base pairs with aromatic chromophore [22]. Here on increasing the amount of DNA in the complex solution resulted in red shift (1.8 nm for n-π* band, Fig.3.5.) and noticeable hypochromicity too, indicating intercalative mode of binding. The intrinsic binding constant (K_b) was evaluated using Wolfe-Shimer equation and the value of K_b was found to be $(2.30 \pm 0.06) \times 10^5 M^{-1}$. Though this value is slightly lower than standard EB ($1.4\times 10^6 M^{-1}$) but mostly higher than other reported Zn(II) complexes [31-33].

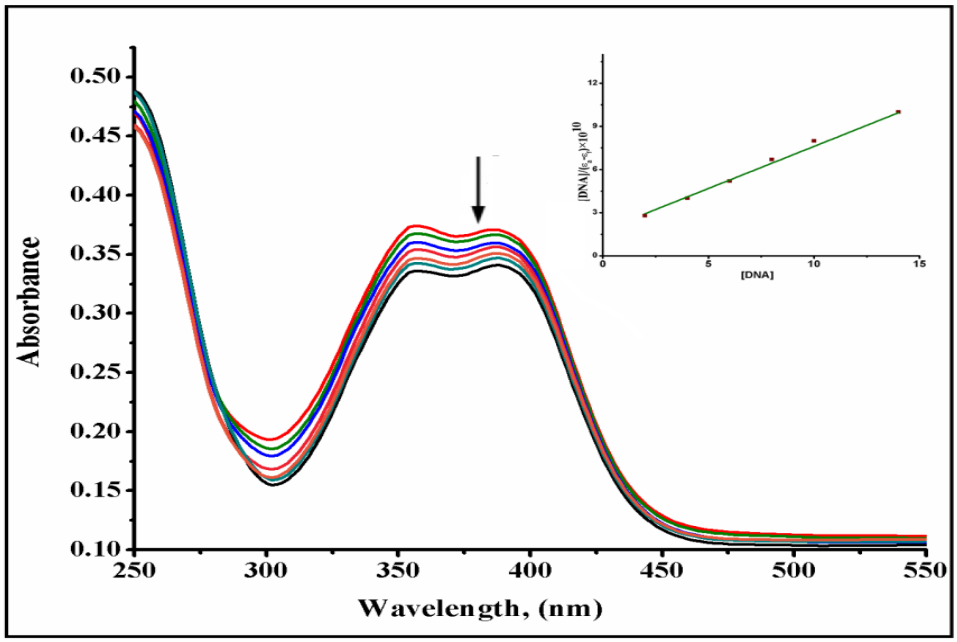

Fig.3.5. Absorption spectra of Zn (II) complex (orange line) in absence and presence of increasing amount of CT DNA (0–15 µM), Inset: plot for binding constant (K_b).

3.3.2.2. Ethidium Bromide (EB) competitive study with fluorescence emission spectroscopy:

Ethidium Bromide (EB)-DNA conjugate exhibit an intense emission band at 592 nm because of intercalation of the planar phenanthridine ring of EB between adjacent DNA base pairs [35]. A significant quenching of the EB-DNA emission band may be observed if a foreign molecule (which can intercalate to DNA equally or stronger than EB) is added into EB-DNA solution [35]. The synthesized Zn(II) complex do not show any emission band in solution or in the presence of CT- DNA or EB when excited at 540 nm. So the observed changes in the emission spectra of EB-DNA solution, when Zn(II)complex is added, are vital to examine the Ethidium Bromide displacement ability of the synthesized complex. The addition of Zn(II) complex in EB-DNA solution causes a significant quenching of the intense emission band at 592nm shown in Fig.3.6. The calculated quenching constant (K_{sv}) value for the synthesized complex is (3.0 ± 0.02) $\times 10^5$ M^{-1} which is mostly higher than other reported Zn(II) complexes [31,34]. Therefore, the observed quenching suggest remarkable ability of Zn(II) complex to displace

intercalator EB from EB-DNA conjugate and divulging indirectly the intercalative mode of binding to DNA [22].

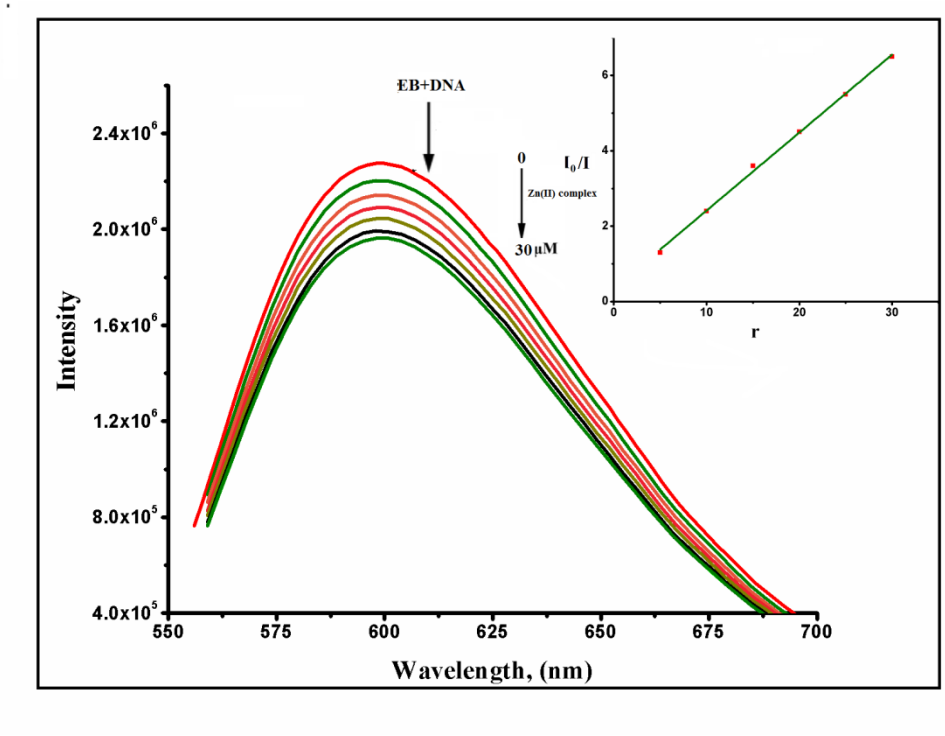

Fig.3.6. Emission spectra of EB bound to the DNA in absence and presence of increasing amount of Zn(II) complex (0–30 µM), Inset: plot for quenching constant (Ksv).

3.3.2.3. Thermal denaturation study:

Thermal denaturation study provides information regarding the extent of intercalation [36]. The intercalation of complex into DNA base pairs generally increases the melting temperature (T_m) of DNA [22]. Fig.3.7. shows thermal denaturization profile of CT-DNA solution both in absence and in presence of Zn(II) complex. The recorded value of T_m for CT-DNA solution was 79.0^0C. But in presence of Zn(II) complex, T_m value increases dramatically to 85.0^0C. These increase in melting temperature of CT-DNA in presence of complex (ΔT_m= 6.0^oC) indicates intercalative binding of Zn(II) complex into DNA [36].

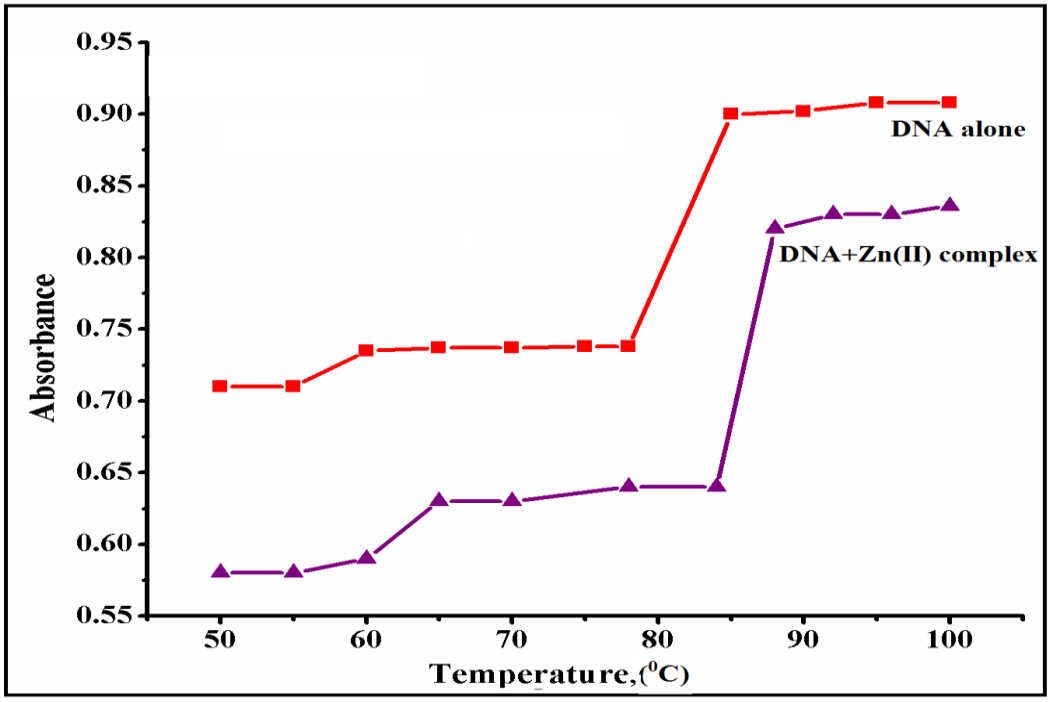

Fig.3.7. Plot of absorbance versus temperature (^{0}C) for the melting of 1) CT DNA alone (red line), 2) CT DNA + Zn(II) complex (purple line).

3.3.2.4. Viscosity measurement:

Viscosity measurement is a substantial tool to study the binding mode of compounds to DNA. The interaction of DNA with metal complexes via intercalation generally results in an increase of the separating distance of the DNA base pairs present at the intercalation site in order to host the binding compound. As a result the length of the DNA helix increases that leads to an increase in DNA viscosity [37]. While in case of binding to DNA via non-classic intercalation (like external groove-binding or electrostatic interaction) results in a kink or bends in the DNA helix. This kink or bends in DNA helix causes slight shortening of the effective length of DNA helix; in such cases the changes in DNA viscosity is less prominent or no change at all [37]. Ethidium bromide is a well known DNA intercalator that increases the relative viscosity of DNA by lengthening the DNA helix. Upon increasing the concentration of Zn(II) complex in the CT-DNA solution, the relative viscosity of DNA

solution increases steadily almost similar to the nature as in case of Ethidium Bromide (shown in Fig.3.8). This increase in viscosity in case of complex solution suggests that the synthesized Zn(II) complex could bind to DNA via intercalation mode which is consistent with the UV-visible and fluorescence spectral data.

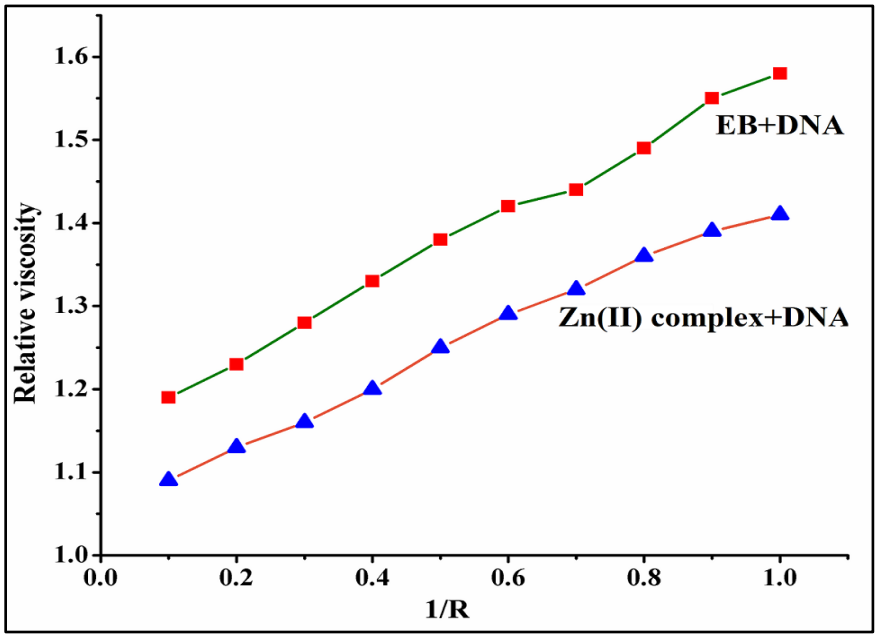

Fig.3.8. Effect of increasing amounts of (a) EB (b) Zn(II) complex on the relative viscosity of CT-DNA.

3.3.2.5. DNA cleavage study:

The DNA cleavage reaction was monitored by gel electrophoresis. To perform cleavage reactions, solutions of pUC19 DNA were prepared and then diluted with loading dye using 1% agarosegel. To each solution obtained, 3 µl of EB (0.5 µg ml−1) was added and mixed well. In the next step, warm agarose was poured and instantly held tightly with a comb to develop sample wells. The gel was placed in an electrophoretic tank and adequate electrophoretic buffers were added to enclose the gel to 1 mm depth. DNA sample (20 µM), 30 µM complex and 10 µMH2O2 in the aforesaid buffer (pH = 7.2) were mixed with a loading dye and filled into the well of the submerged gel using a micropipette. A 50 mA electric current was passed and the gel was taken out from the buffer. The gel was photographically captured under UV light after the completion of

electrophoresis.method with different concentration of Zn(II) complex in presence of H_2O_2. The ability of the complex to cleave DNA is determined by transformation of DNA from supercoiled form (Form 1) to nicked form (Form 2) and linear form (Form 3). For Form I, the fastest migration is observed. If only one strand is cleaved, then Form 1 relaxes to convert into a slower-moving Form II. If both the strands are cleaved, Form 3 is then generated which moves in between Form I and Form II [38]. The result of DNA cleavage is shown in Fig.3.9.

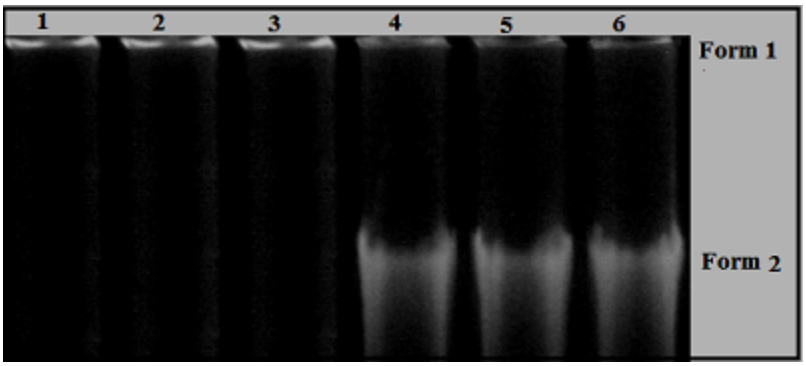

Fig.3.9. Changes in the agarose gel electrophoretic pattern of pBR322 plasmid DNA induced by H_2O_2 for ligand and Zn(II) complex. Lane (1): DNA control, Lane (2): DNA + H_2O_2, Lane (3): DNA+ 10 μM ligand + H_2O_2, Lane (4-6): DNA+ Zn(II) complex + H_2O_2, [complex] = 5, 10, 15μM respectively.

Here for control experiments (lane 1, 2) and in presence of ligand (lane 3), no DNA cleavage is found as there is no metal complex in role while with increasing the concentration of the synthesized complex (lane 4-6), the percentage of Form 1 starts to diminish gradually where as Form II increased. These indicates that the synthesized Zn(II) complex have acted on supercoiled plasmid DNA as there was remarkable difference in bands of the complex compared to band of the control DNA. But in case of ligand there is no appreciable change in the bands with respect to control DNA. The experiment is modulated by hydroxyl radical or peroxo species originated from H_2O_2. The existence of smears in the gel photograph suggesting radical cleavage [39]. The detail mechanism of DNA cleavage by metal complex in presence of H_2O_2 has been reported by various research groups [39,40]. As the synthesized complex is efficient to

cleave the supercoiled plasmid DNA into open circular form, it can be inferred that the complex may inhibit the growth of pathogens by cleaving the genome [24].

3.3.3. Molecular modeling analysis:

3.3.3.1. Swiss target prediction:

The Swiss prediction report for the synthesized Zn(II) complex showed probable association with biological network. It is seen that among the probable targets 20% are enzymes and 40% are cytosolic proteins and there is a huge chunk of another 40% which are unclassified proteins (Fig.2). Among the list of predicted targets there are important compounds such as BCl-2 like protein 1 which are linked to various cellular activities especially pro apoptotic functions. Then again there is Bcl-2-like protein 2 which is also linked to similar function [41]. Apoptosis regulator Bcl-2 is another similar protein which shows interaction with our Zn(II) complex. Induced myeloid leukemia cell differentiation protein Mcl-1 is another protein of BCl-2 family which is essential for apoptosis regulation. All these proteins are essentially related to carcinogenesis pathway [42]. So it is quite likely that the synthesized Zn(II) complex might play a role in general oncology. Moreover, there are other important proteins in this aspect. Microtubule-associated protein Tau promotes microtubule assembly and stability, and might be involved in the establishment and maintenance of neuronal polarity which suggest probable implications in neurodegenerative diseases. They are vital proteins in Alzheimer's disease [43]. These apart important DNA repair enzymes like Tyrosyl-DNA phosphodiesterase 1 and Muscleblind-like protein groups also seems to have some affinity towards the synthesized complex. These multivaried activities suggest importance of the synthesized complex in biological systems.

3.3.3.2. Molecular Docking:

The synthesized Schiff base Zn(II) complex has interesting target partners. To better understand their interaction with the complex and to understand which compound has better interaction we have conducted the molecular docking experiments. Tyrosyl-DNA phosphodiesterase 1 has the best binding affinity with the complex (Table.3.2).

Table. 3.2. Binding affinity of the Zn(II) complex with different proteins:

Protein name	Gene name	PDB ID	Binding affinity(kcal/mol)
Dihydroorotate dehydrogenase (quinone), mitochondrial	DHODH	1d3g	-9.2
Tyrosyl-DNA phosphodiesterase 1	TDP1	1jy1	-10.5
Bcl-2-like protein 1	BCL2L1	1r2d	-9.6
Induced myeloid leukemia cell differentiation protein Mcl-1	MCL1	2nl9	-10
Microtubule-associated protein tau	MAPT	2on9	-7.1
Muscleblind-like protein 1	MBNL1	3d2q	-8.7
Bcl-2-like protein 2 (by homology)	BCL2L2	4cim	-9.4
Apoptosis regulator Bcl-2 (by homology)	BCL2	4lxd	-8.5

These enzymes have DNA repair capacity and catalyze different hydrolysis reactions in nucleotides. Moreover, it is seen earlier from DNA interaction study that the Zn(II) complex has different DNA binding and cleaving activity. So, a high affinity of magnitude -10.5 kcal/mol in autodock enviroment confirms those previous claims. Then again induced myeloid leukemia cell differentiation protein Mcl-1 has the second best binding affinity. This protein plays a major role in apoptotic regulations. It is already seen that apart from Mcl-1 protein different Bcl-2 family proteins has major activity with the synthesized Zn(II) complex. Proteins like Bcl-2-like protein 1, Apoptosis regulator Bcl-2, Bcl-2-like protein 2 are all members of Bcl-2 family of proteins and all have good binding affinity with the synthesized complex (Fig.3.10). The proteins of Bcl-2 family

are all linked to carcinogenesis pathway. So it is confirmed that along from nucleotide interaction the synthesized Zn(II) complex has possible implications in carcinogenesis.

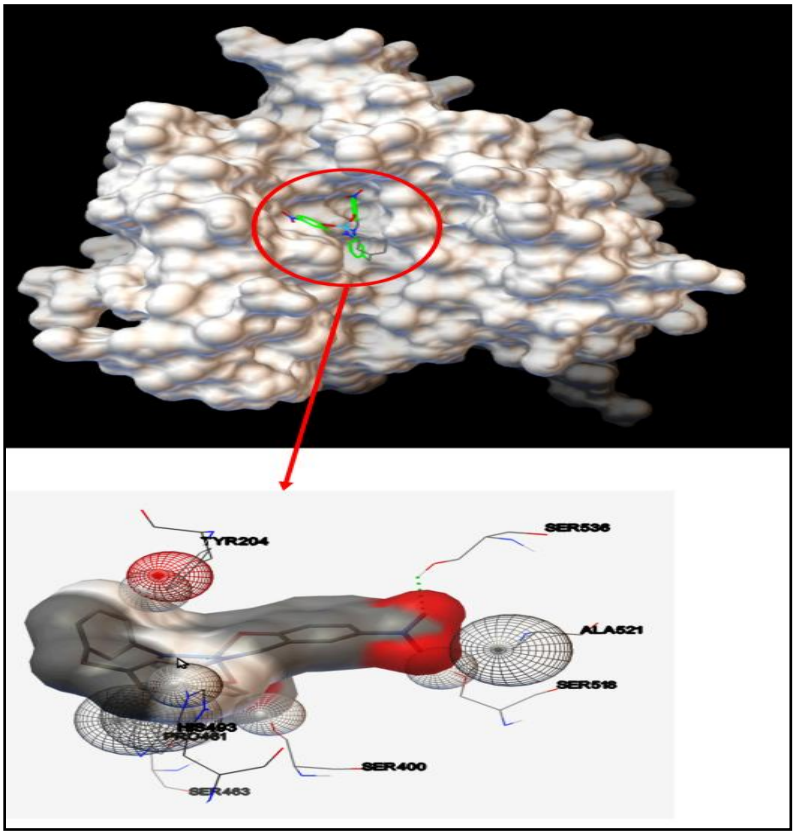

Fig.3.10. Top- The molecular surface view of the protein molecule and the docked complex molecule at its binding site.

3.3.4. In vitro antioxidant activity:

The free radical scavenging activity of Zn(II) complex in dose dependent manner and the differences in the activities compared with standard compound is seen. Half maximal inhibitory concentration (IC_{50}) of Zn(II) complex are shown in the Table.3.3. The synthesized Zn(II) complex showed lower IC_{50} value than ascorbic acid, mannitol, sodium pyruvate, curcumin, quercetin in DPPH, hydroxyl radical, H_2O_2, nitric oxide, superoxide anion, hypochlorous acid scavenging assay and found comparable with peroxinitrate shown by gallic acid and lipid peroxidation shown by trolox [Fig.3.11-Fig.3.15.].

On the other hand, Zn(II) complex showed higher IC_{50} value than lipoic acid and EDTA in singlet oxygen and iron chelation scavenging assay. In case of total antioxidant activity, Zn(II) complex showed better scavenging activity than the standard ascorbic acid. The reducing power of Zn(II) complex was also determined and found that the

Table.3.3. Percentage of inhibition at highest concentration and IC_{50} values (in parentheses) of Zn(II)-Complex and standard for different antioxidant and free radical scavenging assays.

Parameter	Zn(II)-Complex	Standard
DPPH	43.52±0.04**	58.5±0.02
	(272.25±1.06**)	(202.06±0.12)
Nitric oxide	57.43±0.48**	100±0
	(145.42±2.18*)	(60.93±0.04)
Hydroxyl radical	56.9±0.42*	31.31±0.84
	(129.97±1.05*)	(591.48±9.50)
Hydrogen peroxide	25.14±0.6**	7.64±0.68
	(744.25±70.57^{NS})	(2147.45±248.44)
Hypochlorous acid	47.52±0.58*	62.36±0.36
	(214.22±2.13*)	(132.46±4.37)
Peroxynitrite	16.87±0.86^{NS}	17.68±0.21
	(1034.4±65.65*)	(799.39±36.99)
Singlet oxygen	24.81±1.07***	77.97±0.34
	(637.85±36.65**)	(48.43±3.65)
Hemolytic	28.19±0.24**	73.93±1.01
	(440.12±4.85**)	(78.31±2.35)
EMSA	43.49±0.36*	78.67±0.67
	(266.02±0.55***)	(67.03±0.64)

Units in µg/ml. Data expressed as mean±S.D. *-p<=0.05(two sided), **-p<=0.01(two sided), **-p<=0.001(two sided), ^{NS}-p>0.05(two sided)

reducing capacity of Zn(II) complex extract was increased in a dose dependent manner comparable to the reference compound ascorbic acid and ligand.

In the present antioxidant profiling, Zn(II) complex showed potential free radical scavenging activities. The molecule DPPH is a free radical that can accept an electron or hydrogen radical to become stable and reacts with reducing agent to form new bond, changing the color of the solution. The colored DPPH solution mixed with natural

antioxidants. DPPH gives rise to the reduced form with the loss of violet color by the effect of natural antioxidants. Thus, DPPH scavenging activity by Zn(II) complex proves the presence of significant antioxidant properties. But in case of ligand the results are not satisfactory.

Human beings are exposed to H_2O_2 indirectly. Inhibition of H_2O_2 indirectly from environment is rapidly decomposed into oxygen and water and this may produce hydroxyl radicals ($OH^{\cdot}$) that can cause lipid peroxidation and DNA damage in the body. Therefore, the ability of Zn(II) complex to scavenge H_2O_2 proves beneficial for our health.

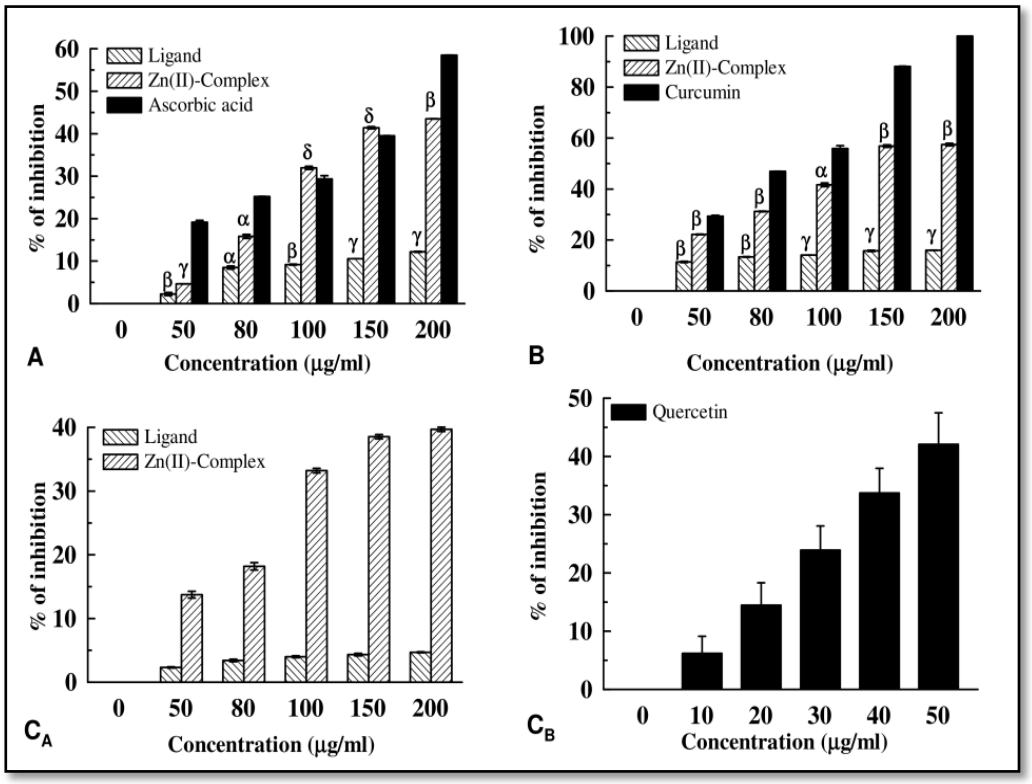

Fig.3.11. Antioxidant activity of Zn(II) metal complex. **(A)** DPPH activity. **(B)** Nitric oxide scavenging activity. **(C)** Super oxide radical scavenging activity. Data expressed as mean ± S.D. $^{\alpha}$ $p<0.05$; $^{\beta}$ $p<0.01$; $^{\gamma}$ $p<0.001$; $^{\delta}$ Non significant when compared with standard.

Nitric oxide plays an important role as pro-inflammatory mediators. Nitric oxide ($NO^{\cdot}$) is synthesized from the amino acid L-arginine by the activation of nitric oxide synthase (NOS). During chronic inflammation iNOS (Calcium independent isoform of NOS) is activated by LPS (Lipopolysaccharide) and produces huge amount of nitric oxide. The active $NO^{\cdot}$ translocate NF-κβ and leads to the formation of cancer. In mitochondria excess amount of nitric oxide reacts with superoxide radical to produce reactive peroxynitrite radical which further causes oxidative stress related disorder. In the present study, it is demonstrated that nitric oxide is down regulated by Zn(II) complex when compared to standard curcumin. Thus, Zn(II) complex might inhibit the inflammation related disorders.

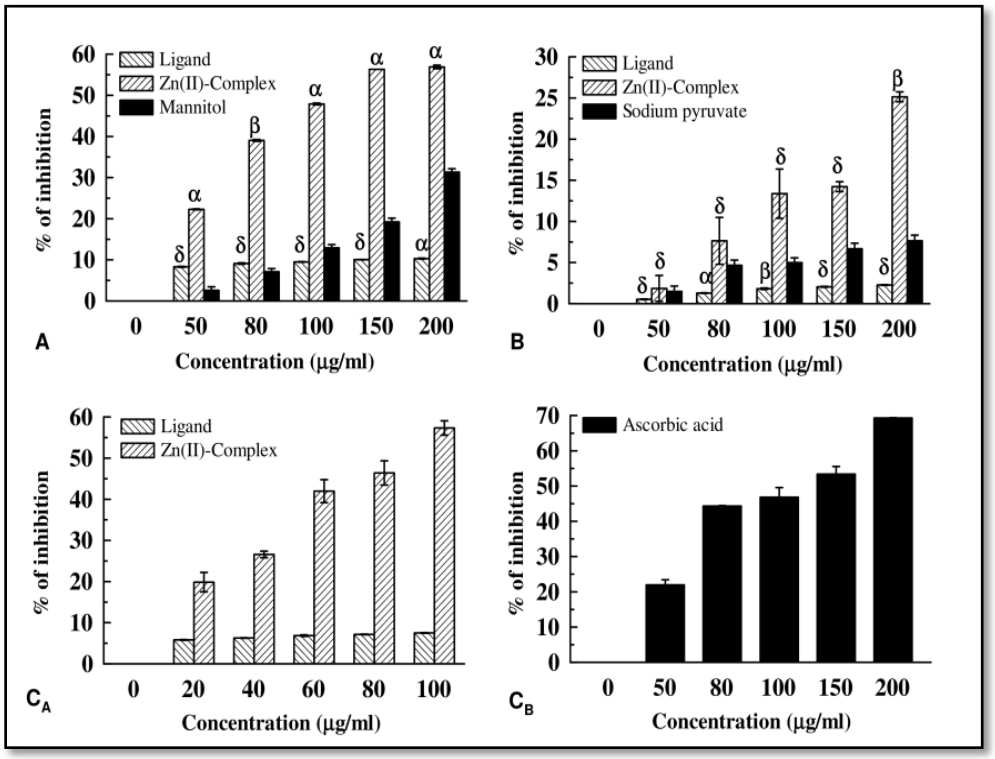

Fig.3.12. Antioxidant activity of Zn(II) metal complex. **(A)** Hydroxyl radical scavenging assay. **(B)** Hydrogen peroxide scavenging activity. **(C)** Total antioxidant scavenging assay. Data expressed as mean ± S.D. * $p<0.05$; ** $p<0.01$; *** $p<0.001$; ^{NS} Non significant when compared with standard.

Hydroxyl radical generated from hydrogen peroxide by Fenton reaction is one of the potent reactive oxygen species in the biological system that react with phospholipids containing polyunsaturated fatty acid moieties of cell membrane and cause damage of cell [44].

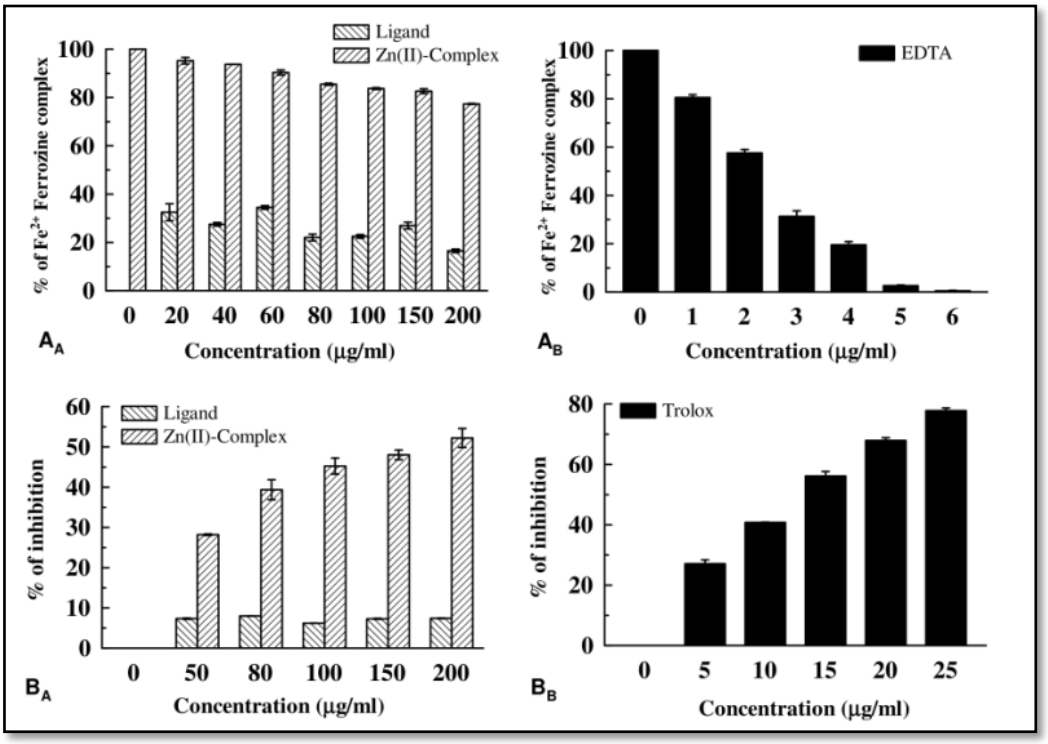

Fig.3.13. Antioxidant activity of Zn(II) metal complex. **(A)** Iron chelation assay. **(B)** Lipid peroxidation activity. Data expressed as mean ± S.D. * $p<0.05$; ** $p<0.01$; *** $p<0.001$; ^{NS} Non significant when compared with standard.

Hypochlorous acid produced from the site of chronic inflammation resulting from the oxidation of Cl^- ion by the neutrophil enzyme, myelo-peroxidase. Hypochlorous acid degrades heme prosthetic group and inactivates the antioxidant enzyme catalase.

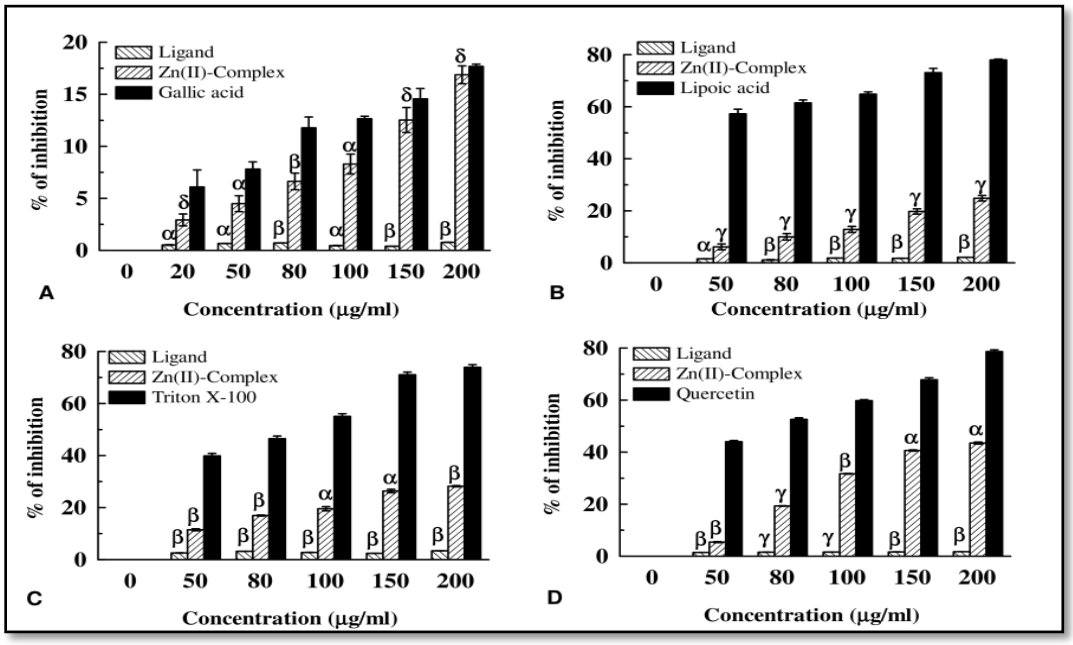

Fig.3.14. Antioxidant activity of Zn(II) metal complex. **(A)** Peroxynitrite scavenging assay. **(B)** Singlet oxygen scavenging assay. **(C)** Hemolytic assay **(D)** Erythrocyte membrane stabilizing activity. Data expressed as mean ± S.D. $^{\alpha}$ $p<0.05$; $^{\beta}$ $p<0.01$; $^{\gamma}$ $p<0.001$; $^{\delta}$ Non significant when compared with standard.

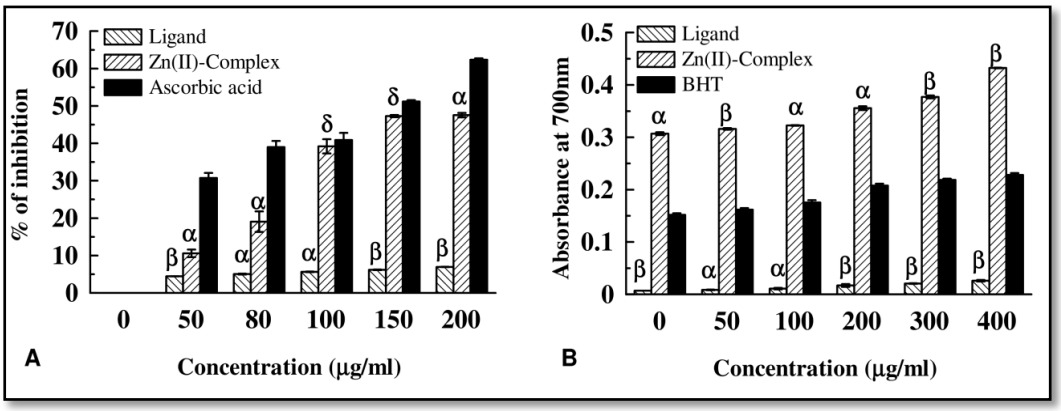

Fig.3.15. Antioxidant activity of Ligand and its Zn(II) metal complex. (A) Hypochlorous acid scavenging assay. (B) Reducing power assay. Data expressed as mean ± S.D. $^{\alpha}$ $p<0.05$; $^{\beta}$ $p<0.01$; $^{\gamma}$ $p<0.001$; $^{\delta}$ Non significant when compared with standard.

Zn(II) complex prove that it has the potentiality to scavenge proxynitrate, hydroxyl radical, superoxide, singlet oxygen and other free radicals too that cause the harmful effect in our biological system. In comparision to the ligand the Zn(II) complex shows far better free radical scavenging activity (Fig. 11 to Fig. 15). Thus, Zn(II) complex might prove to be a key component in prevention of various diseases related to oxidative stress and free radical generation.

3.4. Conclusions:

The synthesized Schiff base ligand and its Zn(II) complex have been characterized by different spectral and analytical techniques. Result of the physical measurements exhibit that the Zn(II) metal ion is coordinated by two azomethine nitrogen and two phenolic oxygen atoms and hence it possibly adopts a tetrahedral geometry. The synthesized complex is stable and non electrolyte in nature. The ability of the synthesized complex to bind to DNA was monitored by different techniques. The experimental results indicate that the Zn(II) complex interacts remarkably with CT-DNA and confirms an intercalative mode of binding to CT-DNA. Apart from high binding affinity with DNA at stable energetics it is also seen that the complex has interaction potential with other biologically important pathways like apoptosis regulation which hints towards possible involvement with Carcinogenesis. In the present study it is also evident that the synthesized complex aided in the recovery of oxidative stress and inhibited lipid peroxidation. On the basis of these facts, antioxidant therapy by synthesized Zn(II) complex alone or in combination with other pharmacological strategies appear as the most reasonable treatment of oxidative stress induced several mental disorders like mental stress, trauma, anxiety etc.

References

1. X. Pei, J. Zhang , J. Liu, *Mol. Clin. Oncol***.** 2014**, 2,** 341–348.

2. P. G. Baraldi, A. Bovero, F. Fruttarolo, D. Preti, M. A. Tabrizi, M. G. Pavani, R. Romagnoli, *Med. Res. Rev*., 2004, **24**, 475–528.

3. B. Rosenberg, L. Van Camp, J. E. Trosko, V. H. Mansour, *Nature*, 1969, **222,** 385–386.

4. Y. Wang, J. Zhou, L. Qiu, X. Wang, L. Chen, T. Liu, W. Di, *Biomaterials*, 2004, **35**, 4297–4309.

5. P. J. Loehrer and L. H. Einhorn, *Ann. Intern. Med.*, 1984, **100**, 704–713.

6. E. R. Jamieson and S. J. Lippard, *Chem. Rev*., 1999, **99**, 2467–2498.

7. E. Meggers, Curr. Opin. Chem. Biol., 2007, **11**, 287–292.

8. M. Kelly, A. Dietrich and S. Gomez-Ruiz, *Organometallics*, 2008, **27,** 4917–4927.

9. M. J. Hannon, *Pure Appl. Chem*., 2007, **79**, 2243–2261.

10. J. Maksimoska, L. Feng, K. Harms, C. Yi, J. Kissil, R. Marmorstein and E. Meggers, *J. Am. Chem. Soc.*, 2008, **130**, 15764–15765.

11. P. Köpf-Maier, *J. Struct. Biol*., 1990, **105**, 35–45.

12. H. Junicke, J. R. Hart, J. Kisko, O. Glebov, I. R. Kirsch and J. K. Barton, *Proc. Natl. Acad. Sci. U. S. A.*, 2003, **100**, 3737–3742.

13. S. Ishida, J. Lee, D. J. Thiele and I. Herskowitz, Proc. *Natl. Acad. Sci. U. S. A.*, 2002, **99**, 14298–14302.

14. K. H. Puthraya and T. S. Srivastava, *J. Inorg. Biochem*., 1985, **25,** 207–215.

15. A. Casini, C. G. Hartinger, C. Gabbiani, E. Mini, P. J. Dyson, B. K. Keppler and L. Messori, *J. Inorg. Biochem*., 2008, **102**, 564–575.

16. S. K. Mal, T. Chattopadhyay, A. Fathima, C. S. Purohit , M. S. Kiran, B. U. Nair, R. Ghosh, *Polyhedron* 2017, **126,** 23–27.

17. M. J. Hannon, V. Moreno, M. J. Prieto, E. Molderheim, E. Sletten, I. Meistermann, C. J. Isaac, K. J. Sanders and A. Rodger, *Angew. Chem., Int. Ed.*, 2001, **40,** 879–884.

18. N. Raman, A. Selvan, S. Sudharsan, Spectrochim. Acta, Part A 2011, **79**, 873.

19. M. P. Kumar, S. Tejaswi, A. Rambabu, V. Kumar, A. Kalalbandi, Shivaraj, Polyhedron 2015, **102**, 111–120.

20. S. Frassinetti, G.L. Bronzetti, L. Caltavuturo, M. Cini, C.D. Croce, J. Environ Pathol Toxicol Oncol 2006, **25**, 597-610.

21. M. Stefanidou, C. Maravelias, A. Dona, C. Spiliopoulou, Archives of Toxicology 2006 80:1.

22. M. Sunita, B. Anupama, B. Ushaiah, C. Gyana Kumari, Arabian Journal of Chemistry 2015.

23. S. Satyanarayana, J.C. Dabroniak, J.B. Chaires, *Biochemistry*, 1992, **31**, 9319.

24. M.A. Neelakantana, F. Rusalraj, J. Dharmaraja, S. Johnsonraja, T. Jeyakumar, M. Sankaranarayana Pillai, *Spectrochimica Acta Part A* 2008, **71**, 1599–1609.

25. B. Hazra, R. Sarkar, S. Biswas, N. Mandal, *Terminalia chebula*, *Terminalia belerica* and *Emblica officinalis*, *BMC Complement. Altern. Med*. 2010, **10**, 20.

26. P. Mahakunakorn, M. Tohda, Y. Murakami, K. Matsumoto, H. Watanabe, *Biol. Pharm. Bull*. 2004, **27**, 38–46.

27. P. Dey, S. Dutta, T.K. Chaudhuri, *J. Pharmaceu. Sci. Inno*. 2013, **2**, 1-4.

28. Sayed M. Abdallaha, Gehad G. Mohamedb,, M.A. Zayed, Mohsen S. Abou El-Ela, *Spectrochimica Acta Part A* 2009, **73**, 833–840.

29. M.M. Omar, G.G. Mohamed, *Spectrochim. Acta (Part A)* 2005, **61,** 929.

30. M. K. Paul, Y. D. Singh, N. B Singh, U. Sarkar, *Journal of Molecular structure*, 2005, **1081**, 316–328.

31. S. Arunagiri, R. Natarajan, M. Liviu, *Monatsh Chem*. 2013, **144,** 605–620.

32. C. J. Dhanaraj, I. Ul Hassan, J. Johnson, J. Joseph, R. S. Joseyphus, Journal of *Photochemistry & Photobiology, B: Biology*. 2016, **162,** 115-124.

33. S. Packianathan, G. Kumaravel, N. Raman, *Appl. Organometal. Chem*. 2017; **31:e3577.**

34. K. P. Chennam, M. Ravi, B. Ushaiah, V. Srinu, R. K. Eslavath, C. Sarala Devi. *J. Fluoresc.* 2016, **26,** 189-205.

35. S. Hazra, A. Paul, G. Sharma, B. Koch, M. Fátima, G da Silva, A. J.L. Pombeiro, *Journal of Inorganic Biochemistry*, **2016**.

36. L. H. Abdel-Rahman, R. M.El-Khatib, L. A. E. Nassr, A. M.Abu-Dief, *Journal of Molecular Structure.* 2013, **1040,** 9–18.

37. M. Tarui, M. Doi, T. Ishida, M. Inoue, S. Nakaike, K. Kitamura, *Biochem. J.* 1994, **304**, 271.

38. D.S. Sigman, *Acc. Chem. Res.*, 1986, **19**, 180-186.

39. K. Yamamoto, S. Kawanishi, *J. Biol. Chem*. 1989, **264**, 15435–15440.

40. Dominique, Desbouisa, Troitsky, P. Ivan, Belousoff, J. Matthew, Spiccia, Leone, Bim, Graham, *Coord. Chem. Rev*. 2012, **256**, 897-937.

41. Gross, Atan, James M. McDonnell, Stanley J. Korsmeyer *Genes & development* 1999, **13.15**, 1899-1911.

42. Frenzel, Anna *Apoptosis* 14.4 (2009): 584-596.Grundke-Iqbal, Inge, *Proceedings of the National Academy of Sciences*. 1986, **83.13**, 4913-4917.

43. Grundke-Iqbal, Inge, *Proceedings of the National Academy of Sciences* 1986, **83.13,** 4913-4917.

44. D. Huang, B. Ou, R.L. Prio, The chemistry behind antioxidant capacity assays, *J. Agric. Food Chem.* 2005**, 53**, 1841–56.